NANOSTRUCTURED ZnO PRODUCED FROM ZnTe FOR RANDOM LASER APPLICATIONS

V. Zalamai[1], A. Burlacu[2], V. Postolache[3], E.V. Rusu[2], V.V. Ursaki[1], and I.M. Tiginyanu[2]

[1]Institute of Applied Physics, Academy of Sciences of Moldova, 5, Academiei str., MD-2028, Chisinau, Republic of Moldova
[2]Institute of Electronic Engineering and Nanotechnologies, Academy of Sciences of Moldova, 3/3, Academiei str., MD-2028, Chisinau, Republic of Moldova
[3]Technical University of Moldova, 168, Stefan cel Mare ave., MD-2004, Chisinau, Republic of Moldova
(Received 13 September 2010)

Abstract

We propose to produce ZnO nanostructured material by thermal treatment in oxygen ambient of bulk ZnTe crystals and nanowires obtained by electrochemical treatment. Bulk ZnTe crystals are transformed into granular ZnO media by thermal treatment in a range of 700–800°C. This technology ensures a high optical quality of the produced ZnO nanostructured material to act as a gain medium for stimulated emission in the ultraviolet spectral region. The produced structures are expected to find applications in microlaser technologies for optoelectronics and photonics.

1. Introduction

Lasing in disordered media (random lasers) has been the subject of intense theoretical and experimental studies since the pioneering work of Letokhov and co-workers [1]. With a wide bandgap of 3.36 eV at room temperature and large exciton binding energy of 60 meV, ZnO holds a great promise for random laser applications provided structures with relevant light scattering properties are produced. Due to the possibility of multiple and switchable growth directions of the wurtzite structure and the high ionicity of its polar surfaces, ZnO provides conditions for the formation of a rich diversity micro/nanostructure ([2-5] and refs therein) many of which may be suitable for lasing.

Remarkable lasing properties were demonstrated with epitaxial and microcrystalline thin films [6-8], arrays of ZnO nanorods [9-19], nanowires [20], nanoneedles [21], nanobelts [22], microdiscs [23], and tetrapods [24-26]. The corresponding emission mechanism was assumed to be related to the near-band-edge radiative recombination of free excitons (FE, ~3.375 eV), exciton-exciton scattering (EES, ~3.18 eV), and electron-hole plasma (EHP, ~3.14 eV) recombination [20]. Note that nanolasers based on ZnO structures are promising for diverse applications including fluorescent sensor technologies, information storage, and microanalysis [9].

Random lasing was mainly demonstrated in ZnO powders and nanocrystalline films. Recently, a new method to produce ZnO random laser media with controlled morphology on the basis of annealing of ZnSe templates has been proposed [27].

In this paper, we show that this approach can be extended to ZnTe templates. In contrast to ZnSe, the as-grown ZnTe crystals are of p-type conductivity, while the ZnO material produced on their basis is of n-type. This approach could open prospects for the development of random laser media with electrical pumping.

2. Technological aspects and morphology characterization

Bulk Na doped ZnTe single crystals with a free hole concentration of $3x10^{18}$ cm^{-3} were used to prepare a nanostructured ZnO material. Two methods were applied. ZnTe bulk crystals were annealed in a temperature interval of 300 to 800°C for 1 h with the first method. The treatment at 800°C produces a nanocrystalline material with the morphology shown in Fig. 1a. The mean grain size of the crystallites is around 300 nm. With a second approach, a template of ZnTe nanowires with a mean diameter around 50 nm (Fig. 1b) is produced in the first step by electrochemical treatment of ZnTe crystals as described elsewhere [28]. The overall dissolution process can be described by the reaction [29]

$$ZnTe + 6h^+ + 2H_2O \rightarrow Zn^{2+} + HTeO_2^+ + 3H^+,$$

where h^+ are holes.

The temperature of the electrolyte was kept constant with a thermostat. The electrolyte was continuously pumped through both chambers of the double cell using a peristaltic pump. The area of the sample exposed to the electrolyte solution was 0.25 cm^2. The anodic etching was carried out in a HNO_3:HCl:H_2O electrolyte with the ratio of 5:20:100 at 25°C with the application of 0.3 s voltage pulses with a frequency of 1 Hz and an amplitude of 5 V. After the etching, the samples were dipped in a solution of polysulfide to remove oxidation products and then rinsed in de-ionized water. The ZnTe nanowires are transformed into ZnO nanowires in the second step by thermal treatment. The morphology of nanowires is not changed by annealing at 500°C, while the material is totally oxidized.

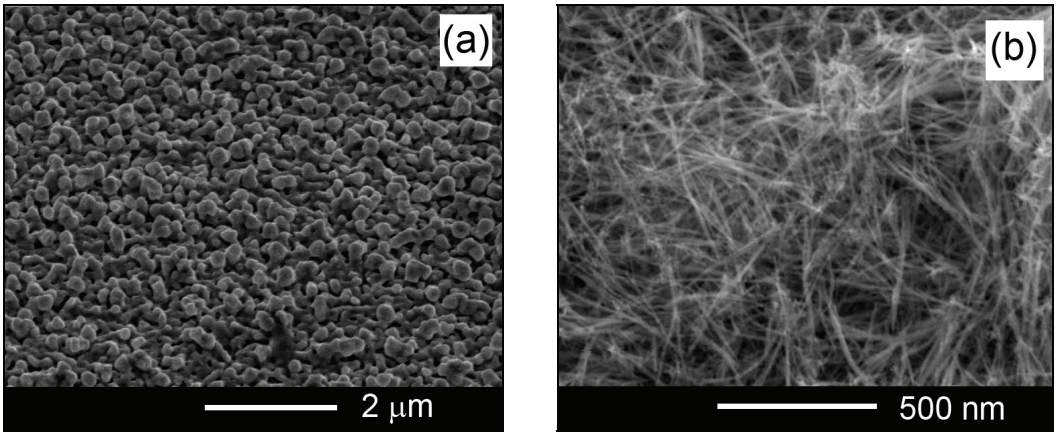

Fig. 1. Morphology of the ZnO nanocrystalline medium produced by thermal treatment from bulk (a) and nanowire (b) ZnTe.

The morphology and chemical composition microanalysis of samples were studied using a VEGA TESCAN TS 5130MM scanning electron microscope (SEM) equipped with an Oxford Instruments INCA energy dispersive X-ray (EDX) system.

3. Photoluminescence and XRD characterization

The continuous wave (cw) photoluminescence (PL) was excited by the 351.1 nm line of an Ar^+ SpectraPhysics laser and analyzed with a double spectrometer ensuring a spectral resolution better than 0.5 meV. The samples were mounted on the cold station of a LTS-22-C-330 optical cryogenic system. The PL spectra were measured at a temperature of 10 K.

Figure 2a demonstrates that the ZnTe material is transformed into high quality ZnO by annealing at 800°C. The as-grown ZnTe sample shows a band-edge emission peak at 2.377 eV related to the recombination of bound excitons followed by two dipper bands at 2.340 eV and 2.314 eV attributed to donor-acceptor pair (DA1) recombination and its LO phonon replica [30]. Apart from near-band-edge emissions, a broad and structured deep-level-related PL band is observed at lower photon energies. This band corresponds to a zero-phonon line at 2.245 eV with a series of phonon replica attributed to another DA2 donor-acceptor pair transition [28]. It was suggested that the excitons observed in these samples are bound to the Na acceptor, since this is a major acceptor impurity in the samples [28]. The Na impurity was also suggested to be involved as acceptor in the two DAP transitions observed, along with two donors with different activation energies [28]. The shallower donor is involved in the DA1 transition, while the deeper one is responsible for the DA2 transition. The high optical quality of the produced ZnO material is demonstrated by the PL spectrum, which is dominated by an emission band related to the recombination of donor bound D^0X, and a band associated with donor-acceptor pair recombination (DA).

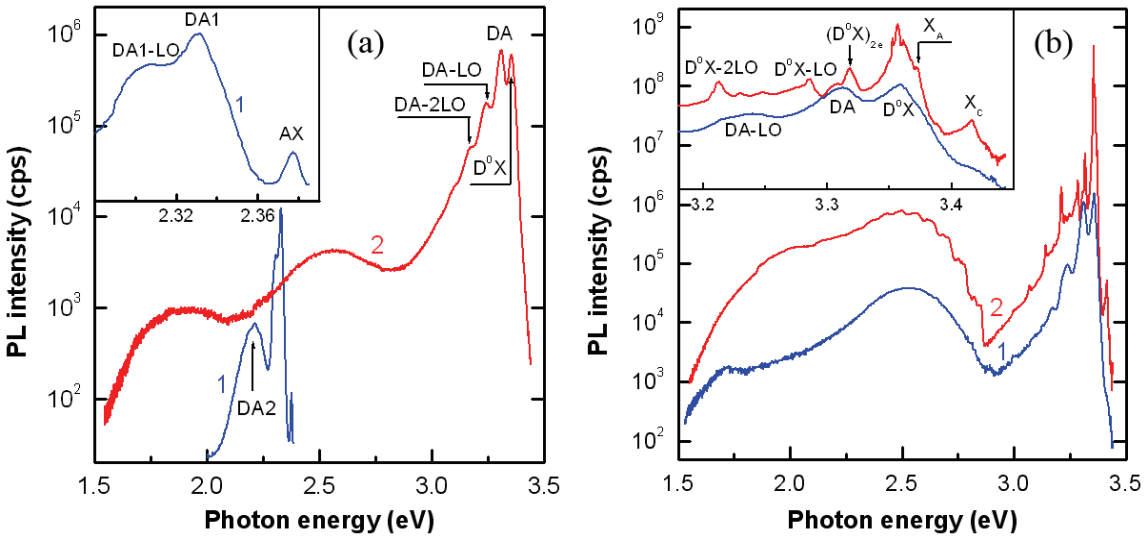

Fig. 2. (a) PL spectra of the initial bulk ZnTe (1) and nanostructured ZnO (2) produced from bulk ZnO through thermal treatment at 800°C, inset is the detailed representation of the near-band-edge emission from bulk ZnTe. (b) A compassion of the PL spectrum of ZnO nanowires produced from ZnTe nanowires (1) with the PL of a high quality ZnO single crystal (2), the inset are the detailed spectra in the near-band-edge region.

The PL and XRD characterization with an X-ray diffractometer with a CuK_α radiation demonstrates that a gradual oxidation of the ZnTe crystal and the transformation of the initial zincblende ZnTe structure to the wurzite ZnO structure occur with increasing the annealing temperature (Fig. 3). Annealing at 400°C leads to the emergence of PL bands related to ZnO crystallites. Only PL bands of the ZnO component remain in the PL spectrum of samples annealed at 700°C. These observations are corroborated by the analysis of XRD spectra (Fig. 3b). The ZnTe crystal annealed at 500°C shows a mixed diffraction pattern of ZnTe and ZnO in the XRD spectrum. The (100), (002), and (101) ZnO diffraction peaks are clearly seen in the XRD spectrum for the sample annealed at 600°C. The XRD pattern for the samples annealed at T_a > 700°C consists of only ZnO diffraction peaks, indicating that ZnTe fully transforms into porous ZnO with a hexagonal wurtzite structure.

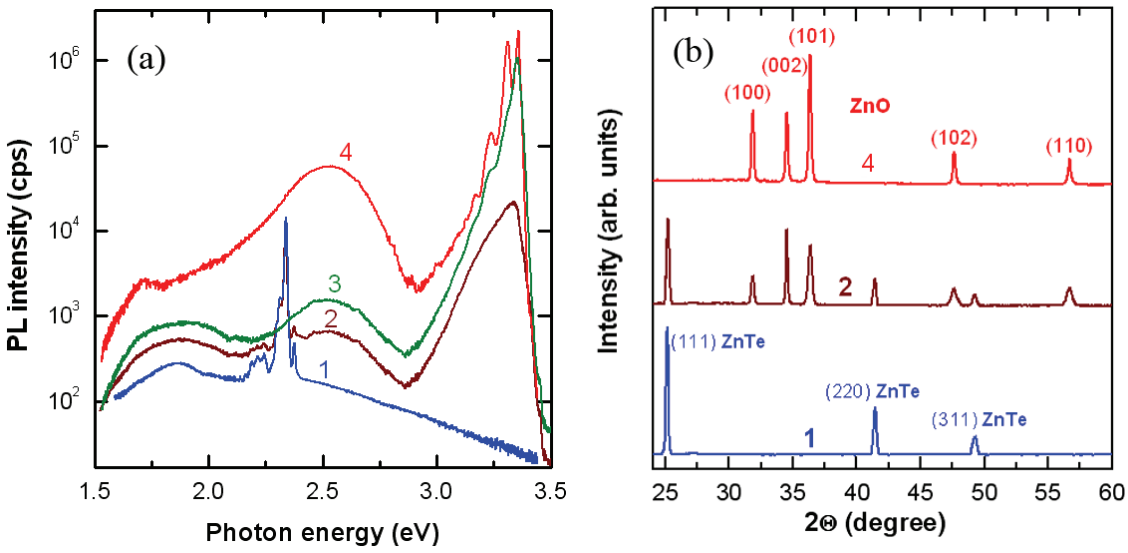

Fig. 3. CW PL (a) and XRD (b) spectra of bulk ZnTe (1) and of the material produced by annealing of bulk ZnTe at 500 (2), 700 (3), and 800°C (4).

Similar transformations occur with ZnTe nanowires, but the temperature of trancormation from ZnTe to ZnO is lower as compared to the bulk material. ZnTe nanowires are totally transformed to ZnO after annealing at 500°C. The high optical quality of the ZnO material produced from ZnTe nanowires is demonstrated by the comparison of its PL spectrum with the spectrum of a high quality ZnO single crystal (Fig. 2b). In both samples, the PL spectrum is dominated by the emission related to the recombination of donor bound D^0X excitons. The only difference is that the spectrum of the material produced from ZnTe nanowires contains a PL band related to the donor-acceptor pair recombination DA with phonon replica, while phonon replicas of the D^0X transition are well resolved in the spectrum of the ZnO single crystal along with the two-electron replica of the D^0X transition $(D^0X)_{2e}$ and the PL band related to the recombination of free excitons X_A and X_C.

4. Characterization of light scattering properties and random lasing effects

The photonic strength of the scattering medium is defined in terms of the transport mean free path l_t, which is the average length required to randomize the direction of propagation of the light by scattering. A small value of l_t corresponds to efficient scattering or high photonic strength. To characterize the photonic strength of the samples, the transport mean-free path l_t is deduced from enhanced backscattering EBS measurements [31]. EBS refers to an increase in the reflected intensity from a disordered multiple-scattering sample at exactly the backscattering direction. This increase is due to interference of waves propagating along time-reversed optical paths. The measured angular dependence of the backscattering ZnO samples with morphologies illustrated in Fig. 1a is shown in Fig. 4a. The full width at half maximum W of the EBS cone is directly related to the transport mean free path l_t. For a non-absorbing and semi-infinite sample, this relation is $l_t = 0.7\lambda(1\text{-}R)/2\pi W$ [32], where R is the angular and polarization-averaged internal reflection at the sample boundary. With the W = 11 mrad and R = 0.75, the determined value of the transport mean free path is $l_t = 1.5$ μm.

The lasing characteristics of the produced ZnO structures were measured at room temperature under the pumping by the third harmonic of a Q-switched Nd:YAG laser (355 nm, 10 ns, 10 Hz). The pumping power density was varied from 0.1 MW/cm^2 up to 6 MW/cm^2.

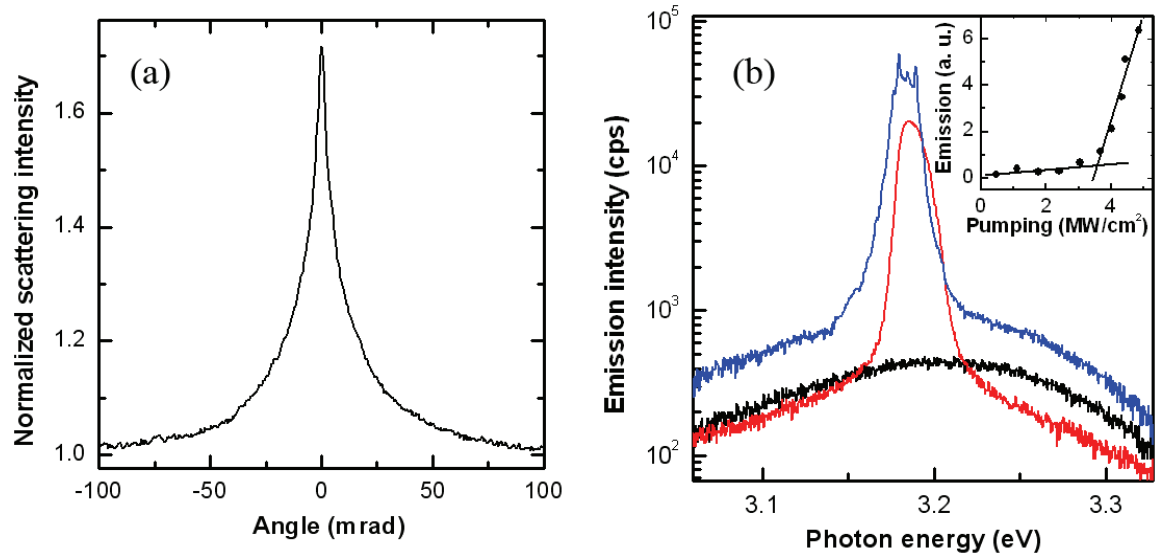

Fig. 4. (a) Measured angular dependence of the backscattering for a ZnO sample with the morphology illustrated in Fig. 1a. (b) Emission spectra of a nanostructured ZnO sample measured at room temperature under the excitation power density of 1.1 MW/cm^2 (1), 4.3 MW/cm^2 (2), and 4.9 MW/cm^2 (3). The spectra are excited by 10 nsec laser pulses and integrated over 30 pulses. The inset is the dependence of the intensity of emission on the excitation power density.

The emission spectra of a porous ZnO sample with the morphology of figure 1a under ns pulse excitation are shown in Fig. 4b. When the pump power reaches a threshold of 3.5 MW/cm^2, the intensity of the emission sharply increases and the emission band is significantly narrowed. Apart from that, a number of narrow lines emerge in the emission spectra with increasing excitation power density. These lines are supposed to be related to lasing modes in random resonators with the highest quality factor.

5. Conclusions

The results of this work demonstrate that a simple thermal treatment of bulk ZnTe crystals and nanowires obtained by electrochemical treatment produces ZnO material of a high optical quality to act as a gain medium for stimulated emission in the ultraviolet spectral region. The thermal treatment of bulk ZnTe crystals provides conditions for the formation of a nanostructured medium with a homogeneous distribution of grains with a mean size around 300 nm. This morphology ensures light scattering properties suitable for random lasing.

Acknowledgments

This work was supported by the Academy of Sciences of Moldova under grant no. 08.817.05.025A.

References

[1] R.V. Ambartsumyan, S.P. Bazhulin, N.G. Basov, and V.S. Letokhov, Sov. Phys.-JETP, 31, 234, (1970).
[2] C. Klingshirn, Phys. Stat. Sol. (b), 244, 3027, (2007).
[3] Z.L. Wang, J. Phys.: Condens. Matter, 16, R829, (2004).

[4] M.C. Newton and P.A. Warburton, Materials Today, 10, 50, (2007).
[5] V.V. Ursaki, E.V. Rusu, A. Sarua, M. Kuball, G.I. Stratan, A. Burlacu, and I.M. Tiginyanu, Nanotechnology, 18, 215705, (2007).
[6] D.M. Bagnall, Y.F. Chen, Z. Zhu, T. Yao, S. Koyama, M.Y. Shen, and T. Goto, Appl. Phys. Lett., 70, 2230, (1997).
[7] M. Kawasaki, A. Ohtomo, H. Koinuma, Y. Sakurai, Y. Yoshida, Z.K. Tang, P. Yu, G.K.L. Wong, and Y. Segawa, Mater. Sci. Forum, 264-268, 1459, (1998).
[8] Z.K. Tang, G.K.L. Wong, P. Yu, M. Kawasaki, A. Ohtomo, H. Koinuma, and Y. Segawa, Appl. Phys. Lett., 72, 3270, (1998).
[9] M.H. Huang, S. Mao, H. Feick, H. Yan, Y. Wu, H. Kind, E. Weber, R. Russo, and P. Yang, Science, 292, 1897, (2001).
[10] Z. Qiu, S. Wong, M. Wu, W. Lin, and H. Xu, Appl. Phys. Lett., 84, 2739, (2004).
[11] T. Okada, K. Kawashima, and M. Ueda, Appl. Phys. A: Mater. Sci. Process., 81, 907, (2005).
[12] Y. Zhang, R.E. Russo, and S.S. Mao, Appl. Phys. Lett., 87, 043106, (2005).
[13] X. Han, G. Wang, Q. Wang, L. Cao, R. Liu, B. Zou, and J.L. Hou, Appl. Phys. Lett., 86, 223106, (2005).
[14] R. Hauschild, H. Lange, H. Priller, C. Klingshirn, R. Kling, A. Waag, H.J. Fan, M. Zacharias, and H. Kalt, Phys. Status. Solidi B, 243, 853, (2006).
[15] A.N. Gruzintsev, A.N. Redkin, G.A. Emelchenko, C. Barthou, and P. Benalloul, J. Opt. A: Pure Appl. Opt., 8, S148, (2006).
[16] A.N. Gruzintsev, A.N. Redkin, Z.I. Makovei, and C. Barthou, Inorg. Mater., 43, 1080, (2007).
[17] A.N. Redkin, Z.I. Makovei, A.N. Gruzintsev, S.V. Dubonos, and E.E. Yakimov, Inorg. Mater., 43, 253, (2007).
[18] V.V. Ursaki et al., J. Phys. D: Appl. Phys., 42, 095106, (2009).
[19] V.V. Ursaki et al., Superlattices and Microstructures, 46, 513, (2009).
[20] H.C. Hsu, C.-Y. Wu, and W.-F. Hsieh, J. Appl. Phys., 97, 064315, (2005).
[21] S.P. Lau, H.Y. Yang, S.F. Yu, H.D. Li, M. Tanemura, T. Okita, H. Hatano, and H.H. Hng, Appl. Phys. Lett., 87, 013104, (2005).
[22] H.D. Li, S.F. Yu, S.P. Lau, and E.S.P. Leong, Appl. Phys. Lett., 89, 021110, (2006).
[23] V.V. Ursaki, A. Burlacu, E.V. Rusu, V. Postolake, and I.M. Tiginyanu, J. Opt. A: Pure Appl. Opt., 11, 075001, (2009).
[24] V.M. Markushev, V.V. Ursaki, M.V. Ryzhkov, et al., Appl. Phys. B: Lasers Opt., 93, 231, (2008).
[25] V.V. Zalamai, V.V. Ursaki, et al., Appl. Phys. B: Lasers Opt., 99, 215, (2010).
[26] V.V. Ursaki, V.V. Zalamai, I.M. Tiginyanu, A. Burlacu, E.V. Rusu, and C. Klingshirn, Appl. Phys. Lett., 95, 171101, (2009).
[27] V.V. Ursaki et al., Semicond. Sci. Technol., 24, 085017, (2009).
[28] E. Monaico, V. Coseac, V.V. Ursaki, N.N. Syrbu, I.M. Tiginyanu, 6th International Conference on Microelectronics and Computer Science, Chisinau, Republic of Moldova, September 24-26, 150, (2009).
[29] F. Zenia, C. Levy-Clement, R. Triboulet, R. Könenkamp, K. Ernst, M. Saad, and M.C. Lux-Steiner, Appl. Phys. Lett., 75, 531, (1999).
[30] N. Lovergine, M. Traversa, P. Prete, K. Yoshino, M. Ozeki, M. Pentimalli, and L. Tapfer, J. Crystal Growth, 248, 37, (2003).
[31] D.S. Wiersma, M.P. van Albada, and A. Lagendijk, Rev. Sci. Instrum., 66, 5473, (1995).
[32] M.B. van der Mark, M.P. van Albada, and A. Lagendijk, Phys. Rev. B, 37, 3575, (1988).